

# Traffic Flow on Single-Lane Road Networks: Multiscale Modelling and Simulation

Alberto De Marchi\*

Matthias Gerdts<sup>†</sup>

2018-05-03

This is a preprint version of the paper

DE MARCHI, GERDTS, Traffic Flow on Single-Lane Road Networks: Multiscale Modelling and Simulation. In: BREITENECKER, KEMMETMÜLLER, KÖRNER, KUGI, TROCH (eds), *9th Vienna International Conference on Mathematical Modelling, IFAC-PapersOnLine*, vol. 51. MATHMOD 2018, Vienna, 2018. DOI: [10.1016/j.ifacol.2018.03.028](https://doi.org/10.1016/j.ifacol.2018.03.028)

## Abstract

This paper addresses the problem of modelling and simulation of the vehicular traffic flow in a road network by adopting a measure-theoretic framework. This allows to describe the system from both, a microscopic and a macroscopic point-of-view simultaneously, in the sense that two scales co-exist and are coupled, namely a set of moving agents and an average density. The resulting mathematical model consists of a strongly coupled PDE-ODE system with non-local interactions. Within this work we specify this multiscale model for a single-lane roundabout, that is, an example of a road network. Then, we focus on the computational aspects in order to develop a setup for numerical simulations and to analyse the results of some experiments. This multiscale simulator can reproduce phenomena that characterize the real physical system, e.g. self-organization effects, and thus it can be adopted as an environment for control algorithms benchmarking or as a tool for simulation-based traffic flow control and optimization.

**Keywords:** Multi-vehicle systems, simulation, modelling and simulation of transportation systems, human factors in vehicular systems.

---

\*Department of Aerospace Engineering, Universität der Bundeswehr München, Neubiberg/Munich, Germany.  
E-MAIL: [alberto.demarchi@unibw.de](mailto:alberto.demarchi@unibw.de), ORCID: [0000-0002-3545-6898](https://orcid.org/0000-0002-3545-6898).

<sup>†</sup>Department of Aerospace Engineering, Universität der Bundeswehr München, Neubiberg/Munich, Germany.  
E-MAIL: [matthias.gerdts@unibw.de](mailto:matthias.gerdts@unibw.de), ORCID: [0000-0001-8674-5764](https://orcid.org/0000-0001-8674-5764).

# 1 Introduction

The complex dynamics of traffic flow stem from and involve the mutual interactions among the vehicles, analogously to crowd and animal group dynamics. These microscopic effects can significantly influence the global evolution, leading to macroscopic self-organization and the emergence of high-level patterns. Mathematical models have been used to quantitatively describe, characterize and predict the behaviour of these systems. Macroscopic information, such as vehicular flow density and flux, is more robust compared to microscopic quantities, such as cars positions and velocities [5]. However, the latter are the major cause of the macroscopic evolution and thus deserve appropriate modelling effort.

Most part of the literature about traffic flow modelling have been emphasizing either scale, neglecting the other. Traffic flow models at the (sub-)microscopic level started and developed from the so-called follow-the-leader models, considering cars as individual agents connected and governed by interaction forces [9, 13], formalized as a system of ordinary differential equations (ODEs). Conversely, macroscopic representations consider the average density of agents and stem from the continuum equation, that is a partial differential equation (PDE). These are typically in the form of first-order models, e.g. the classic work of [14], or second-order models, to analyze particular features, e.g., [16] or to easily account for real traffic data, see [3] for instance. This kind of models has to deal with boundary conditions and, when applied to road networks, with junctions [10, 2], that are a non-trivial (and still open) modeling problem; see, e.g., the work of [12] and the survey paper of [1] and references therein. There are works also in the direction of ODE-based macroscopic models of flows on networks, as well as multi-compartmental models and space-discretization of PDEs, e.g., [11, 15], in order to have less computationally costly models to be used for control purposes. Another technique to build a macroscopic model from the microscopic representation is via the mean-field limit, that has been applied, e.g., to stochastic dynamics of pedestrians and material flow problems [8]. Similar mathematical models and methods have been widely applied to describe and control, e.g., data networks, irrigation channels, logistics and manufacturing processes [1]. Coupled PDE-ODE models have also been adopted to study peculiar traffic conditions, e.g. bottlenecks due to slow vehicles or work zones [6].

Within this work we focus on the multiscale model of vehicular traffic flow, based on the measure-theoretic approach introduced by [18] for crowd dynamics, on a road network; in particular we consider a roundabout as an illustrative example. Self-organization effects have been already observed adopting the same approach in the simple case of the intersection of two roads [5]. The aim of this work is to extend previous results to more complicated networks, without the need of dealing with junctions, by using a model that enables to capture a variety of scales in space and time, depending on the multiscale coupling [4].

The aforementioned coupling of scales may be interpreted as an artifact to model the physical interaction between agents (human drivers or autonomous cars, but also pedestrians or living cells). In practice, a fitting phase may be needed in order to estimate the value of model parameters, such as multiscale coupling and interaction forces. Then, the simulator can be validated by comparing real measurement data to numerical experiments. Finally, these or newly introduced parameters may be treated as control inputs to automatically steer the evolution of

traffic flow as desired. Examples in this direction utilize variable speed limit, ramp meter control and traffic lights [15, 17, 7]. Model-based (or simulation-based) design optimization and real-time traffic flow control are the long-term motivations of this work.

## 2 Methods

This Section introduces the measure-theoretic approach developed by [18] and, specifying a microscopic, a macroscopic and a mixed measure, a continuous-time coupled PDE-ODE model is derived in the context of a single-lane road network. In particular, an interaction kernel among agents is suggested, based on social forces [9, 4] and featuring space-dependent anisotropy. Then, a discrete-time version of the model is presented and the advancing scheme of measures is compared to the push forward used by [4]. The additional space discretization allows to explicit an update scheme for agents' position and average density. Finally, following the work of [4], an algorithm is proposed to collect the main steps needed to simulate the traffic flow evolution.

### 2.1 Multiscale modelling

A general road network with fixed flow direction can be represented by a directed graph composed by a finite set of edges connected by junctions [1]. Let us consider a set of  $N_r$  curves, denoted  $\Omega_r \subset \mathbb{R}^2$ ,  $r \in \mathcal{N}_r = \{1, \dots, N_r\}$ , each one representing a piece of single-lane road. The entire road network is then defined by the union of those curves, namely  $\Omega := \bigcup_{r \in \mathcal{N}_r} \Omega_r$ ; see the illustrative roundabout geometry in Fig. 1. Vehicles, considered as discrete agents or as a continuous flow, move in the road network  $\Omega$ . Thus, their velocity is always tangent to the road where they are moving on; let  $\Omega_t \subset \mathbb{R}^2$  denote the space of feasible velocity vectors associate to  $\Omega$ . Vehicle speed is defined as the component of velocity vector projected on the road, considered positive when in the same direction of expected traffic flow (known a priori); within this work, vehicles always move with non-negative speed.

Let  $t \in \Gamma = [0, T]$  denote time and  $T > 0$  a certain final time. A positive measure  $\mu_t$  is defined such that for any small road segment  $E \subset \Omega$  the number  $\mu_t(E) \geq 0$  gives the number of vehicles contained in  $E$  at time  $t \in \Gamma$ . Given initial condition  $\mu_0$  and appropriate boundary conditions, the continuity equation holds, namely

$$\frac{\partial \mu_t}{\partial t} + \nabla \cdot (\mu_t v) = 0, \quad (t, x) \in \Gamma \times \Omega \quad (1)$$

where  $v : \Gamma \times \Omega \rightarrow \Omega_t$  represents the velocity field transporting the measure  $\mu_t$ . Derivatives in (1) are meant in the functional sense of measures [4]. Boundary conditions for (1) represent how the measure inside the road network interfaces with the one outside. Within this work, network inputs and outputs are not analysed in details, and more investigations are needed to rigorously manage them.

Interaction among vehicles plays a key role in the evolution of  $\mu_t$  and here it is modelled by directly specifying the velocity field  $v$ , and thus obtaining a first order model. This approach is commonly adopted in the literature, especially for macroscopic models [10, 6, 7]. Let the velocity consist of two contributions and be expressed as

$$v(t, x) := v[\mu_t](x) = v_{\text{des}}(x) + \text{proj}_{\Omega_t} \nu[\mu_t](x), \quad (2)$$

the square brackets denoting functional dependence on  $\mu_t$  [4]. Desired velocity  $v_{\text{des}} : \Omega \rightarrow \Omega_t$  is the velocity that agents would set to reach their destination if they did not experience mutual interactions. Instead, interaction velocity  $\nu[\mu_t] : \Omega \rightarrow \mathbb{R}^2$  is the correction that agents make in consequence of the interactions with other vehicles. Projecting  $\nu[\mu_t](x)$  on  $\Omega_t$  is needed in (2) in order to assure a feasible velocity field, namely  $v(t, x) \in \Omega_t$  for any  $(t, x) \in \Gamma \times \Omega$ . Similarly to [4], the interaction contribution affecting the agent placed at point  $x \in \Omega$  is evaluated by adopting the following model:

$$\nu[\mu_t](x) := \int_{\Omega \setminus x} f(\|y - x\|) g(y, x) \frac{y - x}{\|y - x\|} d\mu_t(y), \quad (3)$$

where function  $f : [0, +\infty) \rightarrow \mathbb{R}$  describes the interaction strength based on agents' distance, function  $g : \Omega^2 \rightarrow [0, 1]$  rules the anisotropic aspect of interactions among agents. A model for interaction strength is based on attractive and repulsive (social) forces [9, 5], and, for any  $d > 0$ , it reads:

$$f(d) := \left[ F_a d \, 1_{[0, R_a]}(d) - \frac{F_r}{d} \, 1_{[0, R_r]}(d) \right]_{f_{\min}}^{f_{\max}}, \quad (4)$$

where  $F_a, F_r > 0$  and  $R_a, R_r > 0$  are attraction and repulsion strengths and radii, respectively, and operator  $[\cdot]$  denotes the saturation and it means that the interaction strength  $f(d)$  is restricted to  $[f_{\min}, f_{\max}]$  for any  $d > 0$ . Function  $1_E$  is, for a given set  $E$ , the indicator function of  $E$ , namely  $1_E(x) = 1$  if  $x \in E$ , 0 otherwise. We point out that car length  $L_c$  may be easily embedded into model (4) by evaluating the strength  $f$  on a reduced distance, e.g.  $f(d - L_c)$  instead of  $f(d)$ , holding  $d > L_c \geq 0$ . Function  $g$  is significant because agents see the others in their own (possibly limited) field-of-view; in fact, it reflects the importance of an agent at point  $y$  for one looking from point  $x$ . This aspect is modeled by defining

$$g(y, x) := h(\text{mod}(\alpha(y, x) - \beta(x) + \pi, 2\pi) - \pi), \quad (5)$$

where  $\alpha : \Omega \times \Omega \rightarrow [-\pi, \pi]$  gives the angle between vectors  $y - x \in \mathbb{R}^2$  and  $v_{\text{des}}(x) \in \Omega_t$ ,  $\beta : \Omega \rightarrow [-\pi, \pi]$  is a function that returns the head angle, i.e. the angle between driver's head direction and vehicle velocity (whose direction does not depend explicitly on time). The involved expression in (5) is just to shift the angle  $\alpha(y, x) - \beta(x)$  from  $[0, 2\pi]$  to  $[-\pi, \pi]$ . The contribution  $\beta(x)$  accounts for the space-varying drivers' focus of attention, e.g. on the left when entering into a roundabout with anticlockwise circulation. Also, head direction could depend on the agent's target or planned route (not considered here). Function  $h : [-\pi, \pi] \rightarrow [0, 1]$  carries the anisotropy of the interactions, because agents are not equally sensitive to different directions. Denoting  $\bar{\alpha} \in (0, \pi]$  the angular half-width of the visual field, a simple model for function  $h$  is

$$h(\alpha) := \cos\left(\frac{\pi}{2} \frac{\alpha}{\bar{\alpha}}\right) 1_{[-\bar{\alpha}, \bar{\alpha}]}(\alpha). \quad (6)$$

Finally, we point out that cars indistinguishability, as assumed so far and in the following, is not a restriction and can be overtaken, e.g., [5].

From the microscopic point-of-view, the traffic flow consists of a population of  $N_c$  moving vehicles, whose positions at time  $t$  are denoted by  $P_j(t) \in \Omega$ ,  $j \in \mathcal{N}_c = \{1, \dots, N_c\}$ . At this

micro-scale, each agent can be seen as a Dirac mass in its own position, yielding to the counting measure  $m_t$ , such that

$$m_t(E) := \text{card}\{j \mid P_j(t) \in E\} \quad (7)$$

for any set  $E \subset \Omega$ . Then, introducing the measure  $m_t$  into (1) and exploiting definition (7), a dynamical system of  $N_c$  coupled ODEs is obtained; in fact, it holds [4]

$$\dot{P}_j(t) = v[m_t](P_j(t)), \quad j \in \mathcal{N}_c, \quad (8)$$

where the velocity field is computed through (2)–(6), showing the interactions because of the functional dependence on the measure  $m_t$ .

At the macroscopic level, traffic flow is described as a continuous stream of vehicular mass. Let us consider a macroscopic measure  $M_t$ , absolutely continuous w.r.t. the 1-dimensional Lebesgue measure  $\mathcal{L}$ ,  $M_t \ll \mathcal{L}$ . Then, there exists a function  $\rho(t, \cdot) : \Omega \rightarrow [0, +\infty)$  such that [4]

$$dM_t = \rho(t, \cdot) d\mathcal{L} \quad (9)$$

and, in our context,  $\rho(t, x)$  is meant to describe the traffic density, that is the number of vehicles per unit space, at time  $t$  in the neighbourhood of point  $x$ .

A multiscale approach incorporates both the micro- and macroscopic perspectives. To this end, counting measure  $m_t$  and macroscopic measure  $M_t$  are combined into the definition of a mixed measure, denoted  $\mu_t$ , such that

$$\mu_t(E) := \int_E \theta(x) dm_t(x) + \int_E [1 - \theta(x)] dM_t(x) \quad (10)$$

for any set  $E \subset \Omega$ . Function  $\theta : \Omega \rightarrow [0, 1]$  point-wisely weights the coupling between the two scales, and thus their interactions and effects. In practice, given  $x \in \Omega$ , measure  $\mu_t$  can be interpreted (locally, in the neighbourhood of  $x$ ) as purely macroscopic if  $\theta(x) = 0$  or as purely microscopic if  $\theta(x) = 1$ . Properties of aforementioned micro- and macroscopic measures  $m_t$  and  $M_t$ , Equations (7) and (9) along with (10), entail that the mixed measure  $\mu_t$  can be expressed also as

$$\mu_t(E) = \sum_{\substack{j \in \mathcal{N}_c \\ P_j(t) \in E}} \theta(P_j(t)) + \int_E [1 - \theta(x)] \rho(t, x) d\mathcal{L}(x) \quad (11)$$

for any set  $E \subset \Omega$ . Looking at the interaction velocity  $\nu[\mu_t]$ , from (3), measure  $\mu_t$  makes the overall dynamics not a simple weighted superposition of the individual microscopic and macroscopic dynamics, as pointed out by [4, Section 3.3]. Thus, the model is a strongly coupled PDE-ODE system, unless  $\theta$  is zero or one. In fact, from definitions (3), (7) and (10) along with (9), it follows that

$$\nu[\mu_t](x) = \int_{\Omega \setminus x} \psi(y, x) [1 - \theta(y)] \rho(t, y) d\mathcal{L}(y) + \sum_{\substack{j=1 \\ P_j(t) \neq x}}^{N_c} \psi(P_j(t), x) \theta(P_j(t)) \quad (12)$$

for any  $(t, x) \in \Gamma \times \Omega$ , where for brevity we introduced  $\psi(y, x) := f(\|y-x\|) g(y, x) (y-x)/\|y-x\|$ . If the multiscale parameter  $\theta$  is constant, i.e.  $\theta(x) = \theta^* \in [0, 1]$  for any  $x \in \Omega$ , Equation (12) simplifies and can be expressed in the form:

$$\nu[\mu_t](x) = \theta^* \nu[m_t](x) + (1 - \theta^*) \nu[M_t](x), \quad (13)$$

still maintaining a strong coupling between the scales for any  $\theta^* \in (0, 1)$ .

## 2.2 Discrete-time

Let us introduce a (possibly adaptive) grid for time discretization, i.e. a sequence of time steps  $\{t_n\}_{n \in \mathcal{N}_t}$ ,  $\mathcal{N}_t = \{0, \dots, N_t\}$ , such that  $t_0 = 0$ ,  $t_{N_t} = T$  and  $\Delta t_n = t_{n+1} - t_n > 0$  for any  $n \in \{0, \dots, N_t - 1\}$ . Let us denote  $\mu_n := \mu_{t_n}$  and  $P_j^n := P_j(t_n)$ , for any  $j \in \mathcal{N}_c$ ,  $n \in \mathcal{N}_t$ . By applying the first-order forward Euler method to (8) and rearranging, we obtain an explicit scheme to update vehicles positions, namely

$$P_j^{n+1} = P_j^n + v[\mu_n](P_j^n) \Delta t_n \quad (14)$$

for any  $j \in \mathcal{N}_c$ ,  $n \in \{0, \dots, N_t - 1\}$ . This result has been also formally proved, defining a flow map and neglecting a term  $o(\Delta t_n)$  [4, Section 4], as for the first-order method just applied. Similarly, at the macroscopic level, an advancing scheme for density function  $\rho^n := \rho(t_n, \cdot)$  can be obtained from (1), yielding

$$\frac{\rho^{n+1} - \rho^n}{\Delta t_n} + \nabla \cdot (\rho^n v[\mu_n]) = 0 \quad (15)$$

for any  $x \in \Omega$ ,  $n \in \{0, \dots, N_t - 1\}$ . In order to achieve an explicit update scheme for  $\rho^n$ , it is necessary to introduce a numerical grid for space discretization.

## 2.3 Discrete-space

Let domain  $\Omega$  be partitioned in  $N_s$  pairwise disjoint cells  $E_i \subset \Omega$ ,  $i \in \mathcal{N}_s = \{1, \dots, N_s\}$ . Each cell  $E_i$  is a subset of one and only one curve  $\Omega_r$ ,  $r \in \mathcal{N}_r$ , and it is characterized by a point  $x_i \in E_i$  and a characteristic size  $l_i := \mathcal{L}(E_i) > 0$ . Let density  $\rho^n$  and multiscale parameter  $\theta$  be approximated by piecewise constant functions  $\tilde{\rho}^n$  and  $\tilde{\theta}$ , such that

$$\tilde{\rho}^n(x) = \rho_i^n := \rho^n(x_i) \quad (16)$$

$$\tilde{\theta}(x) = \theta_i := \theta(x_i) \quad (17)$$

for any  $x \in E_i$ ,  $i \in \mathcal{N}_s$ . A simple yet appropriate way to approximate traffic density at any time  $t_n$  is based on the counting measure in a neighbourhood of a point of interest, e.g.

$$\rho_i^n := \frac{\text{card}\{P_j^n \in B_{R_\rho}(x_i)\}}{\mathcal{L}(B_{R_\rho}(x_i))} \quad (18)$$

for any  $i \in \mathcal{N}_s$ ; ball  $B_{R_\rho}(x)$  of radius  $R_\rho > 0$  is adopted to count how many vehicles are in the neighbourhood of  $x$ . Adopting previous definition, piecewise constant macroscopic and mixed measures arise,  $\tilde{M}_n$  and  $\tilde{\mu}_n$ , respectively, such that

$$d\tilde{M}_n = \tilde{\rho}^n d\mathcal{L} \quad (19)$$

$$\tilde{\mu}_n(E) := \int_E \theta(x) dm_n(x) + \int_E [1 - \tilde{\theta}(x)] d\tilde{M}_n(x) \quad (20)$$

for any  $E \subset \Omega$ . Analogously, a piecewise constant  $\tilde{\psi}$  is introduced, such that  $\tilde{\psi}(y, x) = \psi_{ij} := \psi(x_i, x_j)$  for any  $y \in E_i$ ,  $x \in E_j$ ,  $i, j \in \mathcal{N}_s$ , along with  $\tilde{\nu}$ , such that

$$\tilde{\nu}[\tilde{\mu}_n](x) = \int_{\Omega \setminus x} \tilde{\psi}(y, x) [1 - \tilde{\theta}(y)] \tilde{\rho}^n(y) d\mathcal{L}(y) + \sum_{\substack{j \in \mathcal{N}_c \\ P_j^n \neq x}} \psi(P_j^n, x) \theta(P_j^n) \quad (21)$$

for any  $x \in \Omega$ . By using the fact that domain  $\Omega$  has been partitioned into disjoint cells, the integral in (21) can be split, yielding after some manipulations

$$\tilde{\nu}[\tilde{\mu}_n](x) = \sum_{\substack{k \in \mathcal{N}_s \\ k \neq i}} \psi_{ki} (1 - \theta_k) \rho_k^n l_k + \sum_{\substack{j \in \mathcal{N}_c \\ P_j^n \neq x_i}} \psi(P_j^n, x_i) \theta(P_j^n) \quad (22)$$

for any  $x \in E_i$ . Finally, with piecewise constant desired velocity  $\tilde{v}_{\text{des}}$ , such that  $\tilde{v}_{\text{des}}(x) = v_{\text{des},i} := v_{\text{des}}(x_i)$  for any  $x \in E_i$ , a piecewise constant velocity field  $\tilde{v}^n$  can be defined, analogously to (2), such that

$$\tilde{v}^n(x) = v_i^n := v_{\text{des},i} + \text{proj}_{\Omega_t} \tilde{\nu}[\tilde{\mu}_n](x_i) \quad (23)$$

for any  $x \in E_i$ ,  $i \in \mathcal{N}_s$ ,  $n \in \mathcal{N}_t$ . With the piecewise constant approximations just introduced it is possible to find an explicit update scheme for traffic density. In fact, the convective term in (15) can be approximated by the ratio between the net flux through cell  $E_i$  and its size  $l_i$ , namely

$$\frac{\rho_i^{n+1} - \rho_i^n}{\Delta t_n} + \frac{\rho_i^n v_i^n - \rho_{i-1}^n v_{i-1}^n}{l_i} = 0$$

assuming that only flux from cell  $E_{i-1}$  goes (entirely) into  $E_i$ . In the more general case of networks, many fluxes may enter into a cell and each of them may be split among different receiving cells. Let  $\mathcal{P}(i)$  be the set collecting indices of those cells whose flux goes directly into  $E_i$ , i.e.

$$\mathcal{P}(i) := \{k \in \mathcal{N}_s \setminus \{i\} \mid E_i \cap (E_k + B_\epsilon^+(E_k)) \neq \emptyset\}.$$

where ball  $B_\epsilon^+(E)$  is centred at the extreme point of  $E$ , in the traffic flow direction, and it has sufficiently small radius  $\epsilon > 0$ . Let us define also  $\mathcal{P}_+(i) := \mathcal{P}(i) \cup \{i\}$ . Then, let  $\Lambda_{ik}^n \in [0, 1]$ ,  $i, k \in \mathcal{N}_s$ ,  $i \neq k$ , denote the percentage of flux from  $E_k$  going into  $E_i$  at time  $t_n$ . Notice that, by definition, it is  $\Lambda_{ik}^n = 0$  for any  $k \notin \mathcal{P}(i)$ ,  $i \in \mathcal{N}_s$ . Thus, in the case of networks, (15) can be approximated by

$$\frac{\rho_i^{n+1} - \rho_i^n}{\Delta t_n} + \frac{1}{l_i} \left( \rho_i^n v_i^n - \sum_{k \in \mathcal{P}(i)} \Lambda_{ik}^n \rho_k^n v_k^n \right) = 0 \quad (24)$$

for any  $i \in \mathcal{N}_s$ ,  $n \in \{0, \dots, N_t - 1\}$ . By defining  $\Lambda_{ii}^n := -1$  for any  $i \in \mathcal{N}_s$ ,  $n \in \mathcal{N}_t$ , meaning that the flux from a cell is always directed outward the cell itself, the explicit update scheme (24) can be rearranged as

$$\rho_i^{n+1} = \rho_i^n + \frac{\Delta t_n}{l_i} \sum_{k \in \mathcal{N}_s} \Lambda_{ik}^n \rho_k^n v_k^n \quad (25)$$

and also easily written as a matrix-vector multiplication. One could also consider a matrix-valued function  $\Lambda : \Gamma \rightarrow \mathbb{R}^{N_s \times N_s}$ , and denote  $\Lambda^n := \Lambda(t_n)$ , to be used in (25). Matrix  $\Lambda(t)$  would be a representation of the road network topology, with flow directions and splitting, at time  $t$ . Consequently, flow balance has to be a property of matrix  $\Lambda(t)$ , at any time  $t$ , to be consistent and physically meaningful. Neglecting inputs and outputs, the overall matter on the road network does not change in time. Thus, at the macroscopic level, considering (25), it must hold

$$\begin{aligned} 0 &= \tilde{M}_{n+1} - \tilde{M}_n \\ &= \sum_{i \in \mathcal{N}_s} \rho_i^{n+1} l_i - \sum_{i \in \mathcal{N}_s} \rho_i^n l_i \\ &= \Delta t_n \sum_{i \in \mathcal{N}_s} \sum_{k \in \mathcal{N}_s} \Lambda_{ik}^n \rho_k^n v_k^n \\ &= \Delta t_n \sum_{k \in \mathcal{N}_s} \left( \rho_k^n v_k^n \sum_{i \in \mathcal{N}_s} \Lambda_{ik}^n \right) \end{aligned} \quad (26)$$

for any  $n \in \mathcal{N}_t$ , and thus

$$\sum_{i \in \mathcal{N}_s} \Lambda_{ik}^n = 0 \quad (27)$$

for any  $n \in \mathcal{N}_t$ ,  $k \in \mathcal{N}_s$ . However, there is still no unique way to compute the non-zero entries of matrix  $\Lambda(t)$ . Here we propose to consider a concept analogue to density (see Eq. 18), but accounting for the route of each vehicle, that is assumed to be known. Let  $\omega_j \subset \Omega$  denote the curve representing the  $j$ -th vehicle route. As mentioned above, the value of  $\Lambda_{ik}^n$  is the fraction of flux from cell  $E_k$  to  $E_i$  at time  $t_n$ , for any  $i \in \mathcal{N}_s$ ,  $k \in \mathcal{P}(i)$ ,  $n \in \mathcal{N}_t$ ; a mathematical expression could be the following:

$$\Lambda_{ik}^n := \frac{\text{card}\{P_j^n \in B_{R_\Lambda}(x_k) | x_i \in \omega_j\}}{\text{card}\{P_j^n \in B_{R_\Lambda}(x_k)\}}. \quad (28)$$

It should be pointed out that definition (28) is consistent with condition (27), recalling that  $\Lambda_{ii}^n := -1$ ,  $i \in \mathcal{N}_s$ .

In this final part we derive the explicit scheme (25) from a general result proved by [4, Section 5]. Introducing analogue (piecewise constant) approximations, they have shown that

$$\rho_i^{n+1} = \frac{1}{l_i} \sum_{k=1}^{N_s} \rho_k^n \mathcal{L}(E_i \cap \tilde{\gamma}_n(E_k)) \quad (29)$$

for any  $i \in \mathcal{N}_s$ ,  $n \in \{0, \dots, N_t - 1\}$ , where flow map  $\tilde{\gamma}_n$  is such that  $\tilde{\gamma}_n(x) := x + v_i^n \Delta t_n$ , for any  $x \in E_i$ . Considering that cars can move only along the road, for small  $v_k^n \Delta t_n \geq 0$ , Equation (29)



turns into

$$\mathcal{L}(E_i \cap \tilde{\gamma}_n(E_k)) = \mathcal{L}(E_i \cap (E_k + v_k^n \Delta t_n)) \quad (30)$$

$$= \begin{cases} l_i - v_k^n \Delta t_n & k = i \\ v_k^n \Delta t_n & k \in \mathcal{P}(i) \\ 0 & \text{otherwise} \end{cases} \quad (31)$$

This relation is derived by linearization along the curve and neglecting an error depending on  $(v_k^n \Delta t_n)^2$ .

Substituting (31) into (29) and considering matrix  $\Lambda^n$  return exactly the same explicit update equation for density found before, Equation (25). Furthermore, one can notice that the measure cannot return negative values nor values larger than the measure of either the two sets. Thus, given  $n \in \{0, \dots, N_t - 1\}$ , the time step  $\Delta t_n$  has to be sufficiently small to satisfy the condition  $v_k^n \Delta t_n \leq l_i$  for any  $i \in \mathcal{N}_s$ ,  $k \in \mathcal{P}_+(i)$ . Then, among all, it must hold also

$$\Delta t_n \leq \Delta t_n^{\max} = \min_{i \in \mathcal{N}_s} \frac{l_i}{\max_{k \in \mathcal{P}_+(i)} v_k^n}. \quad (32)$$

This is a CFL-like condition similar to the one reported by [4, Theorem 5.1]. In the case of constant space step, i.e.  $l_i = l \ \forall i \in \mathcal{N}_s$ , these two conditions coincide.

## 2.4 Algorithm

This Section sketches an algorithm based on the results obtained so far for the simulation of a multiscale model of traffic flow on road networks. Algorithm 1 is similar to the one reported in [4, Section 5].

## 3 Numerical results

This Section discusses about numerical simulations performed to test Algorithm 1 and results obtained from them. Only few aspects are considered and analysed here, this being just a first step toward the multiscale simulation of traffic flow on road networks. Simulations are carried out into two blocks, using mostly the same set of parameters, that is reported in Table 1. A large roundabout is considered in order to have many cars, in fact  $m_0(\Omega) = M_0(\Omega) = 61$ . To the end of minimizing a source of error discussed later, cars do not exit the roundabout once they are inside and no new cars enter the road network.

### 3.1 Multiscale parameter $\theta$

Firstly, the effect of scales coupling is considered, in the particular case it is uniform on the road network. Starting from the same initial vehicles configuration (uniformly distributed car distance, also on ramps), the evolution is simulated by using different values of the multiscale parameter, namely  $\theta \in \{0, 0.3, 0.7, 1\}$ ;  $\Delta t_n = \min(0.1 \text{ s}, \Delta t_n^{\max})$ ,  $l_i \approx 2 \text{ m}$ . Vehicles positions and

---

**Algorithm 1** Multiscale simulation of traffic flow on road networks.

---

**Input:** Vehicles positions and routes  $\{P_j^0, \omega_j\}_{j \in \mathcal{N}_c}$ .

**Output:** Vehicles positions  $\{P_j^n\}_{j \in \mathcal{N}_c, n \in \mathcal{N}_t}$  and traffic density  $\{\rho_i^n\}_{i \in \mathcal{N}_s, n \in \mathcal{N}_t}$ .

$\theta_i \leftarrow \theta(\cdot), x_i$  for  $i \in \mathcal{N}_s$

// traffic density, (18)

$\rho_i^0 \leftarrow x_i, \{P_j^0\}_{j \in \mathcal{N}_c}, R_\rho$  for  $i \in \mathcal{N}_s$

**for**  $n \leftarrow 0$  **to**  $N_t - 1$  **do**

$\theta_j^n \leftarrow \theta(\cdot), P_j^n$  for  $j \in \mathcal{N}_c$

    // desired velocity

$v_{\text{des},j}^n \leftarrow v_{\text{des}}^n(\cdot), P_j^n$  for  $j \in \mathcal{N}_c$

$v_{\text{des},i}^n \leftarrow v_{\text{des}}^n(\cdot), x_i$  for  $i \in \mathcal{N}_s$

    // interaction velocity, (22)

$\nu_j^n \leftarrow \{P_j^n, \theta_j^n\}_{j \in \mathcal{N}_c}, \{x_i, \theta_i\}_{i \in \mathcal{N}_s}$  for  $j \in \mathcal{N}_c$

$\nu_i^n \leftarrow \{x_i, \theta_i\}_{i \in \mathcal{N}_s}, \{P_j^n, \theta_j^n\}_{j \in \mathcal{N}_c}$  for  $i \in \mathcal{N}_s$

    // velocity, (23)

$v_j^n \leftarrow v_{\text{des},j}^n, \nu_j^n, \Omega_t$  for  $j \in \mathcal{N}_c$

$v_i^n \leftarrow v_{\text{des},i}^n, \nu_i^n, \Omega_t$  for  $i \in \mathcal{N}_s$

    // time step, (32)

$\Delta t_n \leftarrow \{l_i, v_i^n\}_{i \in \mathcal{N}_s}$

    // topology and flows, (28)

$\Lambda^n \leftarrow \{x_i\}_{i \in \mathcal{N}_s}, \{P_j^n, \omega_j\}_{j \in \mathcal{N}_c}, R_\Lambda$

    // vehicles positions and traffic density, (14), (25)

$P_j^{n+1} \leftarrow P_j^n, v_j^n, \Delta t_n$  for  $j \in \mathcal{N}_c$

$\rho_i^{n+1} \leftarrow \rho_i^n, v_i^n, \Lambda^n, \Delta t_n$  for  $i \in \mathcal{N}_s$

---

traffic density at the final time  $t = T$  are depicted in Fig. 1. We point out that there is a fairly continuous transition among the final states predicted by simulations. Also, vehicles positions and density distribution do not always seem to match. We argue that the reason for this is twofold: initialization of density field greatly affects the successive evolution, thus the choice of radius  $R_\rho$  is critical; diverging intersections, i.e. exits, introduce the problem of splitting the vehicular flux, that is quantified through the user-defined radius  $R_\Lambda$ . In order to easily represent the evolution in time, it is useful to track the number of cars and the vehicular mass in each road, see Fig. 2. Looking at the difference between the two measures of vehicular mass (micro- and macro-), one can notice a bias during the final part of the simulation, when no cars are leaving the simulated domain. We argue this is due to the same reasons suggested above.

### 3.2 Computational performances

Scaling properties of computation time have been briefly considered, in particular with a two parameters sweep. Within this block of simulations, it has been set  $\theta = 0.5$ ,  $\Delta t_n = \Delta t$  and  $l_i \approx \Delta x$ , and time and space steps were varied, namely  $\Delta t \in \{0.05, 0.08, 0.1, 0.13, 0.17, 0.2\}$ s and  $\Delta x \in \{1.2, 2, 2.8, 3.6\}$ m. For any choice of  $\Delta t$  and  $\Delta x$  satisfying the CFL-like condition (32), 10

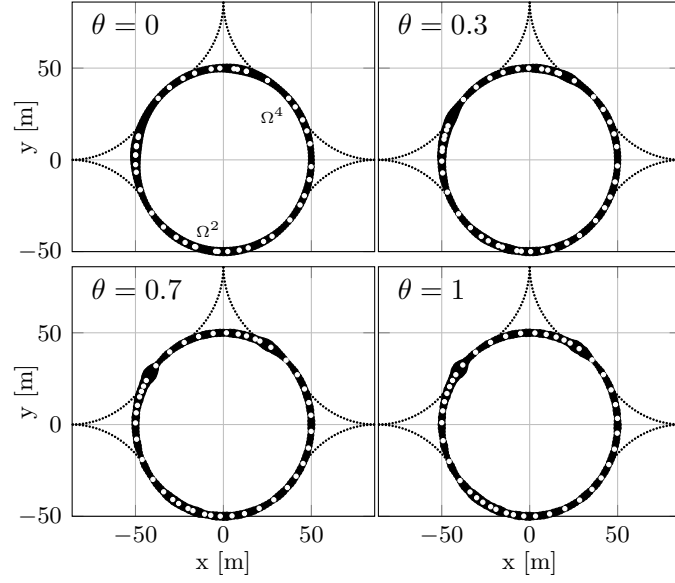


Figure 1: Bird-eye view of vehicles positions (white dots) and scatter plot of traffic density (black), at time  $t = T$ .

different simulations were performed. The result is that the time effort increases linearly with the number of time steps ( $\propto \Delta t^{-1}$ ) and quadratically with the number of space steps ( $\propto \Delta x^{-2}$ ), see Fig. 3.

## 4 Conclusions

In this paper we have presented a measure-based multiscale model of traffic flow in road networks. The two scales are coupled in a mathematically rigorous way because no distinction between them is assumed a priori. We have proposed also an anisotropic interaction model among vehicles, with limited and time-varying field-of-view, and an algorithm that is the numerical counterpart of the presented model. Based on this, simulations have been performed to test the soundness of the approach but only few aspects have been considered and analysed through

Table 1: Simulation parameters.

$R_{\text{round}} = 50 \text{ m}$	$R_{\text{ramp}} = 50 \text{ m}$	$L_c = 4 \text{ m}$
$R_a = 15 \text{ m}$	$F_a = 0.1 \text{ s}^{-1}$	$f_{\text{max}} = 2 \text{ m/s}$
$R_r = 15 \text{ m}$	$F_r = 7 \text{ m}^2/\text{s}$	$f_{\text{min}} = -2 \text{ m/s}$
$\bar{\alpha} = 70^\circ$	$R_\rho = 6 \text{ m}$	$R_\Lambda = 6 \text{ m}$
$v_{\text{des}} = 15 \text{ m/s}$	$\beta = 0^\circ$	$T = 5 \text{ s}$

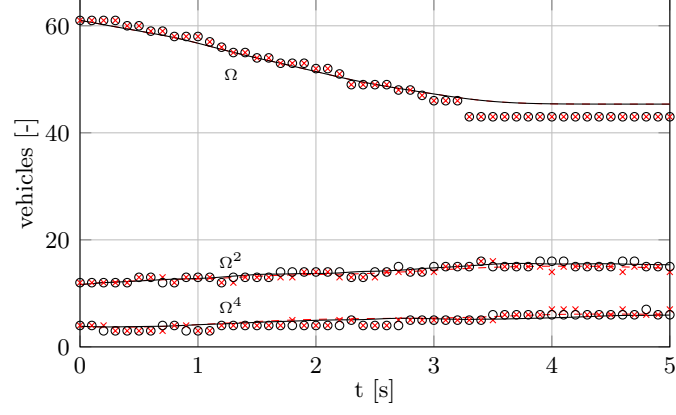


Figure 2: Evolution of micro- (markers) and macroscopic (lines) vehicular mass in time:  $\theta = 0$  (cross, dashed) and  $\theta = 1$  (circle, solid).

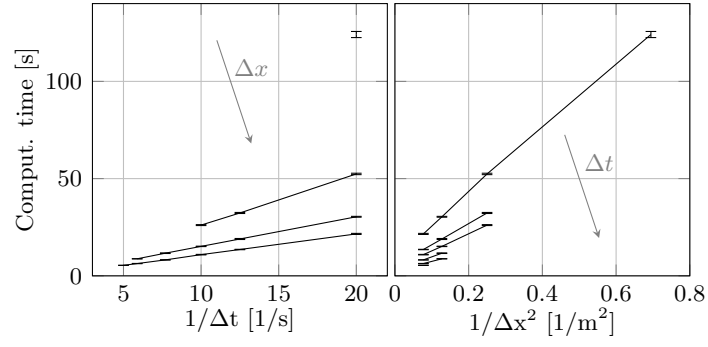


Figure 3: Scaling properties of the computation time.

numerical experiments so far. Further tests need to be performed. However, some steps and parameters that are critical for the simulation have been identified. These limitations define the next steps in the refinement of the model. Moreover, further investigations may face the problem of parameters identification based on traffic data and uncertainty quantification. These to the end of building a tool for benchmarking control algorithms or for model-based control techniques.

## References

- [1] Alberto Bressan, Sunčica Čanić, Mauro Garavello, Michael Herty, and Benedetto Piccoli. Flows on networks: recent results and perspectives. *EMS Surveys in Mathematical Sciences*, 1(1):47–111, 2014.
- [2] Alberto Bressan and Khai T. Nguyen. Conservation law models for traffic flow on a network of roads. *Networks and Heterogeneous Media*, 10(2):255–293, 2015.
- [3] Rinaldo M. Colombo and Francesca Marcellini. A traffic model aware of real time data. *Mathematical Models and Methods in Applied Sciences*, 26(3):445–467, 2016.
- [4] Emiliano Cristiani, Benedetto Piccoli, and Andrea Tosin. Multiscale Modeling of Granular Flows with Application to Crowd Dynamics. *Multiscale Modeling & Simulation*, 9(1):155, 2011.
- [5] Emiliano Cristiani, Benedetto Piccoli, and Andrea Tosin. How can macroscopic models reveal self-organization in traffic flow? In *2012 IEEE 51st IEEE Conference on Decision and Control (CDC)*, pages 6989–6994, 12 2012.
- [6] Maria Laura Delle Monache. Modeling of moving bottlenecks in traffic flow: a PDE-ODE model with moving density constraints. *ESAIM: Proceedings and Surveys*, 45:456–466, 9 2014.
- [7] Paola Goatin, Simone Göttlich, and Oliver Kolb. Speed limit and ramp meter control for traffic flow networks. *Engineering Optimization*, 48(7):1121–1144, 2016.
- [8] Simone Göttlich, A. Klar, and S. Tiwari. Complex material flow problems: a multi-scale model hierarchy and particle methods. *Journal of Engineering Mathematics*, 92(1):15–29, 2015.
- [9] Dirk Helbing. Traffic and related self-driven many-particle systems. *Reviews of Modern Physics*, 73(4):1067–1141, 2001.
- [10] M. Herty and A. Klar. Modeling, simulation, and optimization of traffic flow networks. *SIAM Journal on Scientific Computing*, 25(3):1066–1087, 2003.
- [11] M. Herty, A. Klar, and A.K. Singh. An ODE traffic network model. *Journal of Computational and Applied Mathematics*, 203(2):419–436, 2007.

- [12] Michael Herty, S. Moutari, and M. Rascle. Optimization criteria for modelling intersections of vehicular traffic flow. *Networks and Heterogeneous Media*, 1(2):275–294, 2006.
- [13] S P Hoogendoorn and P H L Bovy. State-of-the-art of vehicular traffic flow modelling. *Proceedings of the Institution of Mechanical Engineers, Part I: Journal of Systems and Control Engineering*, 215(4):283–303, 2001.
- [14] M. Lighthill and J. Whitham. On kinematic waves. *Proc. R. Soc. Lond.*, 229(A):281–345, 1955.
- [15] S. Lin, B. De Schutter, Y. Xi, and H. Hellendoorn. Fast Model Predictive Control for Urban Road Networks via MILP. *IEEE Transactions on Intelligent Transportation Systems*, 12(3):846–856, 9 2011.
- [16] S. Moutari, M. Herty, A. Klein, M. Oeser, B. Steinauer, and V. Schleper. Modelling road traffic accidents using macroscopic second-order models of traffic flow. *IMA Journal of Applied Mathematics*, 78(5):1087–1108, 2013.
- [17] Legesse Lemecha Obsu, Maria Laura Delle Monache, Paola Goatin, and Semu Mitiku Kassa. Traffic flow optimization on roundabouts. *Mathematical Methods in the Applied Sciences*, 38(14):3075–3096, 2015.
- [18] Benedetto Piccoli and Andrea Tosin. Time-evolving measures and macroscopic modeling of pedestrian flow. *Archive for Rational Mechanics and Analysis*, 199(3):707–738, 3 2011.